Rupert, C. S. (1960), *J. Gen. Physiol. 43*, 573.
Rupert, C. S. (1962a), *J. Gen. Physiol. 45*, 703.
Rupert, C. S. (1962b), *J. Gen. Physiol. 45*, 725.
Rupert, C. S. (1964), *in* Photophysiology, Vol. II, Giese, A. C., Ed., p 283.
Rupert, C. S., Goodgal, S. H., and Herriott, R. M. (1958), *J. Gen. Physiol. 41*, 451.
Saito, N., and Werbin, H. (1969a), *Photochem. Photobiol. 9*, 389.
Saito, N., and Werbin, H. (1969b), *Radiation Botany 9*, 421.
Setlow, J. K., and Boling, M. E. (1963), *Photochem. Photobiol. 2*, 471.
Setlow, R. B. (1968), *Progr. Nucleic Acid Res. Mol. Biol. 8*, 272.
Sutherland, B. M., and Sutherland, J. C. (1970), *Biophys. J. 9*, 1329.
Terry, C. E., and Setlow, J. K. (1967), *Photochem. Photobiol. 6*, 799.
Trosko, J. E., and Mansour, V. H. (1969), *Mutation Res. 7*, 120.
Van Baalen, C. (1968), *Plant Physiol. 43*, 1689.
Wacker, A., Dellweg, H., and Jacherts, D. (1962), *J. Mol. Biol. 4*, 410.
Wacker, A., Dellweg, H., and Weinblum, D. (1960), *Naturwissenschaften 47*, 477.
Webb, J. L. (1966), Enzymes and Metabolic Inhibitors, Vol. II, New York, N. Y., Academic, p 642.
Werbin, H., and Rupert, C. S. (1968), *Photochem. Photobiol. 7*, 225.
Wildner, G. F., and Criddle, R. S. (1969), *Biochem. Biophys. Res. Commun. 37*, 952.

Subunit Structure of L-Aspartate β-Decarboxylase from *Alcaligenes faecalis**

William F. Bowers,† Valentine B. Czubaroff, and Rudy H. Haschemeyer

ABSTRACT: Sedimentation equilibrium studies of highly purified L-aspartate β-decarboxylase from *Alcaligenes faecalis* show the molecular weight of the 19S holoenzyme to be 675,000. The 19S apoenzyme obtained by resolution at pH 5–6 undergoes dissociation at pH 8.0 to a 6S component which is one-sixth as large as the holoenzyme and is itself composed of two polypeptide chains. The morphological appearance of the holoenzyme revealed by electron microscopy of negatively stained preparations is presented and compared with that expected for possible dodecameric structures.

For this purpose a versatile computer program has been developed to simulate negative staining of macromolecules under a variety of conditions.

L-Aspartate β-decarboxylase from *Alcaligenes faecalis* has been intensively investigated by Meister and coworkers (Novogrodsky *et al.*, 1963; Soda *et al.*, 1964; Novogrodsky and Meister, 1964a,b; Wilson and Meister, 1966; Tate and Meister, 1968, 1969a,b; Tate *et al.*, 1969) with respect to various catalytic and chemical properties of the enzyme. Tate and Meister (1968) demonstrated that the highly purified 19S holoenzyme migrates as a single band on acrylamide gel electrophoresis, and that the resolved apoenzyme dissociates at pH 8 into a 6S component of increased electrophoretic mobility.

Spectrophotometric and optical rotatory dispersion titration studies (Wilson and Meister, 1966) indicated that approximately 1 mole of pyridoxal-5′-P is bound per 52,000 g of enzyme, consistent with earlier minimal pyridoxal-5′-P unit values of 53,000 and 57,000 (Novogrodsky and Meister, 1964a) from microbiological and phenylhydrazone procedures, respectively. Tate *et al.* (1969) found that about 1 mole of β-chloro-L-alanine could be bound per 60,000 g of enzyme in their studies on active-site labeling. This level of binding was also required to totally inactivate the enzyme. The enzyme contains 11 methionine, and 49 lysine and arginine residues per 50,000 g (Tate and Meister, 1968), and cyanogen bromide cleavage yields 12 peptides, while trypsin digestion results in about 43 fragments (M. Jensen, unpublished data). These results are in accord with the view that the enzyme contains a unique amino acid sequence with a total molecular weight of about 50,000–60,000, identical with that required per coenzyme binding site.

We report here the results of sedimentation equilibrium molecular weight studies on the 19S, 6S, and totally dissociated forms of L-aspartate β-decarboxylase from *A. faecalis*. Electron microscopic studies on the enzyme are presented

* From the Department of Biochemistry, Cornell University Medical College, New York, New York 10021. *Received February 5, 1970.* The electron microscopic investigation reported here was initiated at Tufts University School of Medicine and V. B. C. is grateful to that institution for a Summer Medical Student Fellowship award. Supported by grants from the U. S. Public Health Service (HE-11822) and the National Science Foundation (GB-7042).

† Supported by Public Health Predoctoral Fellowship 1-F01-GM-40,809.

and are discussed in terms of likely models for molecular symmetry. Analog images are obtained by computer simulation of negative staining.

Experimental Section

Materials. Spectral Grade Ultra Pure guanidine hydrochloride was obtained from Mann Research Laboratories. Glutaraldehyde was prepared by dilution to 0.5% from fresh vials of 8% aqueous electron microscopic grade material obtained from Polysciences, Inc. L-Aspartate β-decarboxylase, prepared as described by Tate and Meister (1968), was generously supplied by Dr. Suresh Tate.

Analytical Ultracentrifugation. Instrumentation and procedures used in our laboratory for concentration difference (ΔC) and meniscus depletion sedimentation equilibrium studies have been described previously (Zelazo and Haschemeyer, 1969). The ΔC analysis was used in early stages of this work before electronic speed control had been installed on the Model E ultracentrifuge employed. The modest macromolecular gradients extending to the meniscus were required to prevent convective disturbances under those conditions.

Convective disturbances were also occasionally noted in meniscus depletion experiments on the large 19S enzyme even after installation of the electronic speed control. Therefore, a modification (Bethune and Simpson, 1969) of the moderate-speed equilibrium method (LaBar, 1965) was employed for confirmatory molecular weight determinations on the holoenzyme. Speeds and concentrations for the moderate speed runs were selected to give a final gradient at the column base of about 40 fringes/mm in the cell, our current limit of resolution (Haschemeyer and Bowers, 1970), and a concentration of the meniscus, C_m, of from 10 to 40% that of the initial concentration, C_0. The experiments were conducted essentially as described for the meniscus depletion method, except that in this case the rotor was oversped initially to deplete the meniscus, and then the relaxation of protein back to the meniscus was followed photographically with time after deceleration to the equilibrium speed. Absolute concentration is then readily obtained from the fringe shift between the initial "at speed" depleted photograph and the one obtained at sedimentation equilibrium. The integral fringe shift at a reference radial level was confirmed by comparison of "at speed" and final equilibrium achromatic photographs.

Sedimentation coefficients were calculated from photoelectric scanning patterns as the rate of movement of the 50% boundary position. Symmetry of the boundary was evaluated from probability plots as described by Markham and Reichmann (1962) cited in Markham (1967). The RTIC system was calibrated for each rotor using a National Bureau of Standards thermometer. Temperatures were determined after careful confirmation of the reported ice point, using the emergent stem and tabular corrections supplied by the Bureau. RTIC readings were taken after each run using the calibration stand to confirm conductivity of the mercury cup. Speeds were computed from odometer readings. Corrections for solvent viscosity and density were estimated from the International Critical Tables (1926) and the data of Kawahara and Tanford (1966).

Electron Microscopy. The methods employed in our laboratory for negative staining have been described previously (Haschemeyer, 1968, 1970). Most recently, we have preferred ultra-thin carbon as the support film and have obtained through-focal series in 500-Å intervals. A Philips EM200 microscope was used at an accelerating potential of 80 or 100 kV and the manufacturer's anticontamination device is now routinely employed.

Negative Stain Analogs. The computer simulation studies were begun with a program similar in principle to the superposition projection method developed by Finch and Klug (1967) for simulation of negatively stained images of icosahedral viruses. The results presented here were generated by a more elaborate program developed recently to compute a more realistic two-dimensional stain analog image.[1] Normal input parameters include coordinates of the center of the molecule and the center of each subunit sphere, the radius of the spheres, the thickness of the negative stain embedding sheet, and a scaling factor. The program computes a stain thickness density map by deleting from each map location all volume elements above it that are found to be less than a radius distance from the center of any subunit. A dot of light whose size is inversely proportional to stain thickness is ultimately created at each map coordinate on the CRT screen (there are 25 raster units on the 11 × 14 in. screen per map coordinate) resulting in a half-tone composite analog image.

Additional *a priori* conditions may be readily imposed upon a structure simulated by this method. Entering a radius value greater than half the center-to-center distance of contacting subunits creates bonding domains throughout the molecule which are broader than single-point contacts. A provision has also been made to link specific pairs of subunits, creating dimers which appear either as prolate ellipsoids or as "dumbbells." For this purpose the pairs of subunits to be linked are specified along with the radius of a linking sphere. The program assigns this sphere center coordinates computed to place it midway between the linked subunit pair. Stain thicknesses less than the diameter of the molecule may be used to simulate bottom staining only. Finally, the program has a provision to enter the radius of an additional central sphere which may be used to simulate lack of stain penetration into the hollow core of a shell structure.

Results

Analytical Ultracentrifugation. The 19S holoenzyme and the 6S apoenzyme (Tate and Meister, 1969a) each migrate as a single sharp boundary in sedimentation velocity experiments (Figure 1A,B). These boundaries are symmetrical as judged by the linearity of probability plots over the region from 2.5 to 95% of the total concentration across the boundary. Although on standing longer than a few hours at pH 8, the 6S apoenzyme begins to lose competence to reassociate

[1] Computations were performed on the IBM 360-75/91 computer at the Columbia University Computer Center. The FORTRAN-IV program generates metalanguage output by means of the Integrated Graphics Software (IGS) system developed by Stromberg Datagraphics, Inc. and the Rand Corp. Microfilm copy of the graphic CRT display is subsequently obtained from the Stromberg Datagraphics S-C 4060 system.

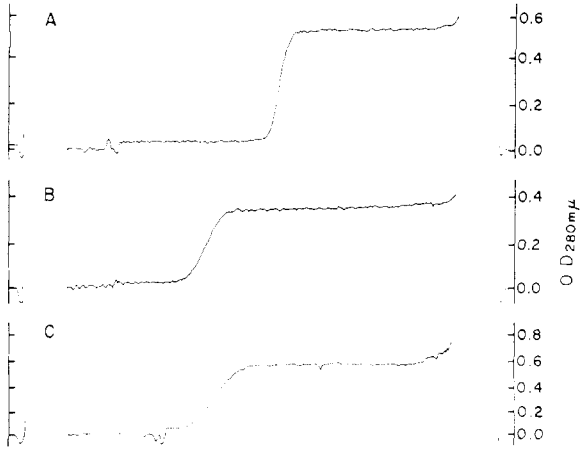

FIGURE 1: Sedimentation velocity of the principal enzyme forms. The capital letters identify the components as described in Table I. Experiments were conducted at 24° with an initial concentration of 0.4–0.6 mg/ml. The photoelectric scanner patterns A, B, and C were taken 15, 29, and 80 min, respectively, after reaching a nominal speed of 59,780 rpm.

to the 19S form by either addition of pyridoxal-5′-P (Tate and Meister, 1968) or by dialysis to pH 5.5 buffer, its physical properties (*i.e.*, sedimentation coefficient, electrophoretic mobility, and molecular weight) remain unchanged for long periods of time.

Dialysis of the apoenzyme at 24° against 5 M guanidine hydrochloride, 2 mM mercaptoethanol, and 0.05 M Tris-acetate titrated to pH 8.0 results in further dissociation and unfolding to a 1.6S component which sediments as a single boundary (Figure 1C). The probability plot of this pattern showed only slight deviation from linearity, perhaps reflecting the effect of restricted diffusion near the meniscus upon

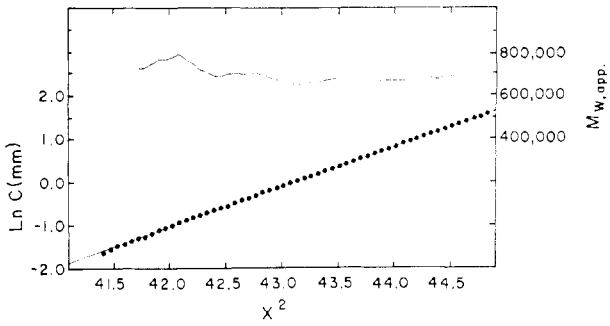

FIGURE 2: Sedimentation equilibrium of the 19S holoenzyme (moderate-speed method of LaBar (1965) and Bethune and Simpson (1969)). The left and right extremes of the abscissa correspond to the radial positions of the meniscus and base of the column, respectively. Concentration is in millimeters displacement on the plate (1.2 mm is equivalent to 1.0 mg/ml). The line represents the least-squares slope of all the data points. $M_{w,app}$ as a function of X^2 is computed from the least-squares slope of an 11-point interval for the midpoint of each interval, and these values are plotted above as a connected line function. A value for $M_{w,app}$ of 672,000 was obtained in this particular run from the least-squares slope of all points excluding those near the meniscus which deviate from linearity as seen from the derivative function. The data were obtained at 4790 rpm at an initial protein concentration of 1.2 mg/ml in pH 5.5 acetate buffer (Table I).

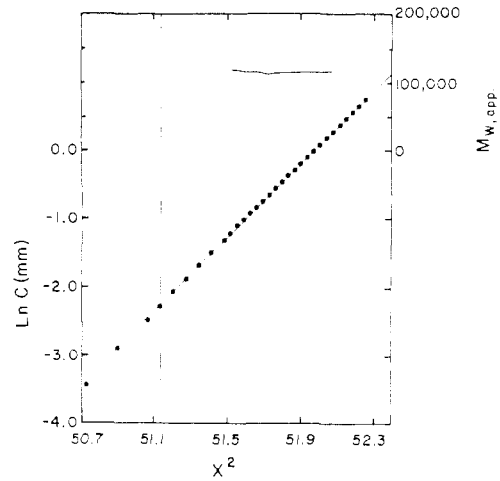

FIGURE 3: Sedimentation equilibrium of the 6S apoenzyme (meniscus depletion method of Yphantis (1964)). The vertical line designates the first point included in the least-squares calculation, corresponding to a displacement of 0.1 mm. The right-hand extreme of the abscissa represents the solution base. The 11-point derivative is computed and plotted as described in Figure 2. The speed was 19,995 rpm and initial protein concentration was 0.23 mg/ml in pH 8 Tris buffer (Table I).

such a slowly sedimenting species, and/or the presence of significant S *vs.* C dependence.

The sedimentation equilibrium analysis of a typical LaBar (1965) moderate-speed run on the holoenzyme is seen in Figure 2. The nonlinearity of $M_{w,app}$ near the meniscus region probably reflects a small error in the determination of the meniscus concentration, but the effect of this error becomes negligible at the higher concentrations present over the bottom half of the column. Computer simulation of sedimentation equilibrium distributions under the conditions shown for Figure 2 but with contamination by varying amounts of dimer or "$^1/_6$-mer," the most likely contaminants anticipated, were made to evaluate the limits of the method in detecting heterogeneity. These studies revealed that such contaminants present at concentrations of 5% or more would have been detected above experimental noise as upward curvature in the value of the apparent weight-average molecular weight, $M_{w,app}$, obtained by moving derivative analysis. No such curvature was detected and it may therefore also be concluded that the enzyme is homogeneous to well within the limits required for the ΔC analysis to give a reliable estimate of the apparent Z-average molecular weight (Zelazo and Haschemeyer, 1969).

Figure 3 shows a similar analysis for a typical Yphantis (1964) meniscus depletion equilibrium experiment on the 6S form of the apoenzyme. The noise level of the moving derivative is typical for the results obtained on this species and only slightly superior to those obtained on the 1.6S component run at higher speed in guanidine hydrochloride. Again, we estimate that a 5% contaminant with a molecular weight differing from the principal component by two or more would have been readily detected, and the ΔC data are therefore reliable for the 6S and 1.6S forms of the enzyme as well.

No reliable method is available in our laboratory for determining density increments (*e.g.*, see the review by Casassa

TABLE I: Ultracentrifugal Analysis of L-Aspartate β-Decarboxylase from *A. faecalis*.

Enzyme Form	$s_{20,w}$ (S)	M_{app}[d]		
		ΔC	Meniscus Depletion	LaBar
A. Holoenzyme[a]	19.00	679,500		652,000
	19.01	669,700		672,100
	18.73	679,800		673,900
		689,600		
	Mean	678,600	Mean	
	18.9 ± 0.2		675,000 ± 11,000	
B. Apoenzyme[b]	5.78	113,200	114,200	
	5.83	118,200	111,500	
	5.76	111,800	116,400	
	Mean		Mean	
	5.79 ± 0.04		114,000 ± 2,600	
C. Guanidine hydrochloride dissociated apoenzyme[c]		61,040	56,230	
		58,630	56,990	
		59,800	58,200	
	1.63 ± 0.03		Mean	
			58,500 ± 1,800	

[a] In 0.05 M sodium acetate, 1 mM Na_2EDTA, and 0.1 M NaCl, titrated to pH 5.5 with acetic acid. [b] In 0.05 M Tris, 1 mM Na_2-EDTA, and 0.1 M NaCl, titrated to pH 8.0 with acetic acid. [c] In 5 M guanidine hydrochloride, 0.05 M Tris, and 2 mM mercaptoethanol, titrated to pH 8.0 with acetic acid. [d] Average values obtained for each experiment as described in the Experimental Section and in the legends to Figures 2 and 3.

and Eisenberg, 1964) on the limited quantity of enzyme available. Consequently, the partial specific volume was calculated from amino acid composition and found to be 0.738; this value was taken for all species in calculating molecular weights and correcting sedimentation velocity data to standard conditions. A summary of these results is presented in Table I.

The ratio of molecular weights for the 19S to 6S form of the enzyme (5.92) demonstrates that L-aspartate β-decarboxylase is composed of six 6S subunits. The fact that preferential binding should be quite negligible (and similar for the two forms) in the solvents used, the degree of homogeneity of the samples, and the error analysis of the molecular weight data exclude the nearest alternatives, 5 and 7, from consideration. The molecular weight ratio of 1.95 for the 6S to 1.6S species could be subject to rather severe error due to preferential binding of solvent components to the latter form. However, the nearest whole-number alternatives to 2 (1 and 3) for the number of 1.6S components/6S apoenzyme are considerably out of the range of expected deviations in molecular weight due to such an error in $\bar{V}$. We conclude that L-aspartate β-decarboxylase is composed of twelve 1.6S components, assembled by secondary association of six dimers.

Electron Microscopy. A typical electron micrograph of the holoenzyme negatively stained with uranyl oxalate is shown in Figure 4. The most common recognizable regular presentations are an apparent hexameric cluster, a triad cluster (both marked by stain penetration of the center), and an apparent tetrameric cross. Fixation of the molecules, application of the sample with a high-pressure spray gun, and use of other negative stains are among the many variations of the negative staining technique employed during the course of this study. None produced a significant increase in morphological detail. It is necessary to conclude, therefore, that either the results presented here are representative of realistic projections of the enzyme structure or that some uniform detrimental artifact is encountered during specimen preparation and is unlikely to be readily circumvented by further experimentation. The unlikelihood of such a consistently uniform artifact of preparation favors the view that many of the presentations seen in the micrographs reflect true morphological detail of a more complex molecular architecture than has heretofore been interpreted for a dodecameric protein.

Discussion

Subunit Composition of L-Aspartate β-Decarboxylase. Molecular weight data presented in the Results section may be combined with the binding and chemical data cited in the introduction to provide a more complete description of the enzyme. All attempts to dissociate the protein into a smaller particle of molecular weight less than 57,000 (one-half the molecular weight of the more accurate value for 6S apoenzyme) were unsuccessful. This result and the peptide mapping data establish that L-aspartate β-decarboxylase is composed of 12 identical (or nearly identical) polypeptide chains with a molecular weight of about 57,000.

Results of binding with pyridoxal-5′-P and β-chloro-

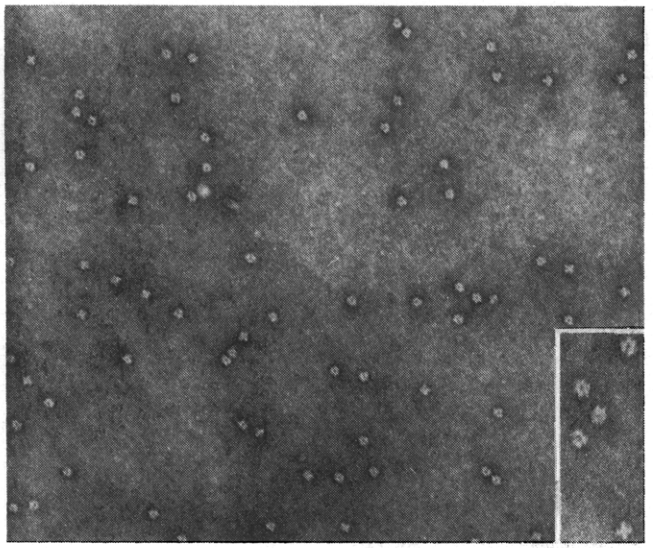

FIGURE 4: Aspartate β-decarboxylase negatively contrasted with uranyl oxalate at pH 6.8. Apparent diameter of the molecule is 150 ± 10 Å under all staining conditions as judged by comparison with the spacing of catalase crystals photographed at the same magnification. The micrograph was taken sufficiently near focus to assure that the observed images reflect specimen contrast. Despite the high resolution, no further meaningful detail is visible at higher magnification as seen in the inset.

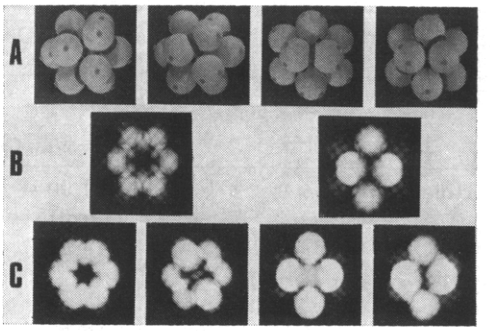

FIGURE 5: The compact dodecameric tetrahedral model assembled from six isologous dimers. (A) Successive views of the model from left to right along a threefold axis, a pseudo-threefold axis, a twofold axis, and a pseudo-twofold axis, respectively. Each isologous intradimer domain is denoted by a ring, and the complementary heterologous binding sets by disks punched from identically colored Velcro tape and glued to the spheres with the aid of a jig at the appropriate angles. (B) Negative stain analog simulation of the various principal regular orientations assuming spherical subunits and a stain sheet thickness four times the subunit diameter. Note the images along the twofold and threefold axes are indistinguishable from those of their respective pseudo axes. (C) Simulation as in part B but with isologous dimers linked by a sphere of diameter 0.9 that of the subunits.

L-alanine are in good agreement with a model for the enzyme in which each of the 12 polypeptide chains contains an "active site," and in which all sites are enzymatically active as suggested by the data of Tate *et al.* (1969), which indicates that approximately 12 moles of bound β-chloro-L-alanine is required before all enzymatic activity has been eliminated.

Independent confirmation of the results presented here demonstrating that the 19S enzyme is composed of six dimeric units is provided by the mixed-reconstitution experiments of Tate and Meister (1970) employing L-aspartate β-decarboxylase from *A. faecalis* and from *Pseudomonas dacunhae*. Reassociation of an equimolar mixture of 6S apoenzyme obtained from these two bacteria resulted in a reconstitution mixture which migrated on acrylamide gel electrophoresis as seven evenly spaced bands. The mobilities of the fastest and slowest moving components were identical with those of the respective parent holoenzymes. These results, described in detail by Tate and Meister (1970), would seem to require that both enzymes have identical or nearly identical quaternary geometry and that both contain six apoenzyme subunits per molecule.

Possible Symmetry of the Enzyme. In order to interpret the molecular weight data and electron micrographs in terms of possible symmetry models, we make the reasonable assumption that the twelve subunits of L-aspartate β-decarboxylase are arranged in the molecule so as to be spatially equivalent (Monod *et al.*, 1965; Hanson, 1966).

We know of only two general dodecameric symmetry classes which may be assembled from isologous dimers, which approximate the observed morphology in some details, and which maintain spatial equivalence of all subunits. The more easily visualized class is the dihedral (D_6) hexagonal model suggested by Valentine *et al.* (1968) for the symmetry of *E. coli* glutamine synthetase. This group potentially includes all orientations from the one observed in the *E. coli* enzyme, in which the subunits of both rings are in near register, through all relative rotational intermediates of the rings about the D_6 axis of angles up to 30° in either direction. In addition, there is no *a priori* requirement that the subunits be spherical.

The negatively stained images for a D_6 dodecamer with spherical subunits (*e.g.*, those obtained with *E. coli* glutamine synthetase) are inconsistent with those observed here for L-aspartate β-decarboxylase in that tetrameric crosses (rather than squares) and trimers are not expected for the dihedral model. Consideration of anticipated images for nonspherical subunits, for partial ring staggering, and for linked dimers (*i.e.*, little stain penetration at the dyad axis) in a staggered configuration is only slightly more satisfying.

The other dodecameric model which requires consideration is the tetrahedral shell class. There are multiple geometrical alternatives for the arrangement of six dimers in the tetrahedral shell model (*e.g.*, any orientation between an "extended" and a "compact" one). The compact extreme (Figure 5A), in which a second pair of complementary heterologous trimer binding sets exist on the surface of each protomer, represents a logical end point in evolution in the manner discussed by Monod *et al.* (1965) and by Hanson (1966) for the "pseudo-tetrahedral" D_2 tetramer. By analogy, this model might be termed "pseudo-icosahedral." Computer simulations of expected electron microscopic images of this model oriented along the three- and twofold axes, and totally engulfed in negative stain are seen in Figure 5B. Figure 5C shows the expectations for the compact model with linked dimers joined by a more extensive isologous domain.

Both the tetrameric cross and hexagonal presentations observed in electron micrographs of L-aspartate β-decarboxylase closely approximate expectations for the compact tetrahedral shell. The trimer presentation can readily result

from projections along a threefold axis in which some excess trimer contrast is introduced by virtue of more predominant bottom staining.

An even better approximation to the observed morphology might be possible if the tetrahedron were constructed from dimers with an axial ratio other than 2. An increase in the dimer axial ratio results in less correlation between observed and expected results, but a relative contraction of the major axis of the dimer may well improve the correlation. In the limit as the dimer axial ratio approaches unity the model is morphologically indistinguishable from a dihedron with two stacked trimer rings in a maximally staggered configuration (pseudo-D_3). A hexamer and a tetrameric appearing cross would result from projections down the three- and twofold axes, respectively. Again, the trimer presentation would result from incomplete engulfment by the negative contrasting medium.

We therefore favor a closed-shell tetrahedral model similar to that shown in Figure 5 as the most probable quaternary structure of L-aspartate β-decarboxylase.

Acknowledgment

We thank the Departments of Anatomy at Tufts University School of Medicine and Cornell University Medical College for generously providing time on their electron microscopes.

References

Bethune, J. L., and Simpson, R. T. (1969), *Fed. Proc. 28*, 1520.
Casassa, E. F., and Eisenberg, H. (1964), *Advan. Protein Chem. 19*, 287.
Finch, J. T., and Klug, A. (1967), *J. Mol. Biol. 24*, 289.
Hanson, K. R. (1966), *J. Mol. Biol. 22*, 405.
Haschemeyer, R. H. (1968), *Transactions, N. Y. Acad. Sci., Ser. II, 30*, 875.
Haschemeyer, R. H. (1970), *Advan. Enzymol. 34* (in press).
Haschemeyer, R. H., and Bowers, W. F. (1970), *Biochemistry 9*, 435.
International Critical Tables of Numerical Data, Physics, Chemistry and Technology (1926), National Research Council, New York, N. Y., McGraw-Hill.
Kawahara, K., and Tanford, C. (1966), *J. Biol. Chem. 241*, 3228.
LaBar, F. E. (1965), *Proc. Natl. Acad. Sci. U. S. 54*, 31.
Markham, R. (1967), *Methods Virol. 2*, 287.
Monod, J., Wyman, J., and Changeux, J.-P. (1965), *J. Mol. Biol. 12*, 88.
Novogrodsky, A., and Meister, A. (1964a), *J. Biol. Chem. 239*, 879.
Novogrodsky, A., and Meister, A. (1964b), *Biochim. Biophys. Acta 85*, 170.
Novogrodsky, A., Nishimura, J. S., and Meister, A. (1963), *J. Biol. Chem. 238*, PC1903.
Soda, K., Novogrodsky, A., and Meister, A. (1964), *Biochemistry 3*, 1450.
Tate, S. S., and Meister, A. (1968), *Biochemistry 7*, 3240.
Tate, S. S., and Meister, A. (1969a), *Biochemistry 8*, 1056.
Tate, S. S., and Meister, A. (1969b), *Biochemistry 8*, 1660.
Tate, S. S., and Meister, A. (1970), *Biochemistry 9*, 2626.
Tate, S. S., Relyea, N. M., and Meister, A. (1969), *Biochemistry 8*, 5016.
Valentine, R. C., Shapiro, B. M., and Stadtman, E. R. (1968), *Biochemistry 7*, 2143.
Wilson, E. M., and Meister, A. (1966), *Biochemistry 5*, 1166.
Yphantis, D. A. (1964), *Biochemistry 3*, 297.
Zelazo, P. O., and Haschemeyer, R. H. (1969), *Biochemistry 8*, 3587.